Chandler period variations due to solar activity

Yavor Chapanov[1], Cyril Ron[2] & Jan Vondrák [2]

[1]Climate, Atmosphere and Water Research Institute, Bulgarian Academy of Sciences

[2]Astronomical Institute of Czech Academy of Sciences

yavor.chapanov@gmail.com, ron@asu.cas.cz, vondrak@ig.cas.cz

Introduction

The solar activity affects terrestrial systems by means of direct radiation over Earth surface, influences charged particles of the solar wind, and the solar magnetic field. The solar wind directly affects Earth magnetic field, ionosphere and atmosphere. The **sunspot numbers (SSN)** represent both **Total Solar Irradiance (TSI)** and solar wind variations. The SSN and TSI variations are highly correlated in decadal period bands, less correlated in the annual bands.

The variations of solar magnetic field represented by the **North-South solar asymmetry (N-SSA)** modulate the solar wind. Variations of TSI, SSN and N-SSA affect ocean and atmosphere, whose variations cause Chandler wobble excitation. *So, we may expect significant solar influence on Chandler wobble variations, expressed by strong correlation in selected frequency bands between Chandler period value and any of solar activity indices – TSI, SSN or N-SSA.*

Data and Methods used

The solar activity variations are presented by indices of SSN, N-SSA and TSI. The SSN sunspots have been observed during the last 4 centuries, while the observations of TSI are available only for the last decades. The last version of estimated TSI for the last 400 years is based on the NRLTSI2 historical TSI reconstruction model by J. Lean (Kopp et al., 2016; Lean, 2000, 2010; Coddington et al., 2015). The TSI and SSN data are presented in Fig.1. The daily and annual values of SSN are provided by the Royal Observatory of Belgium.

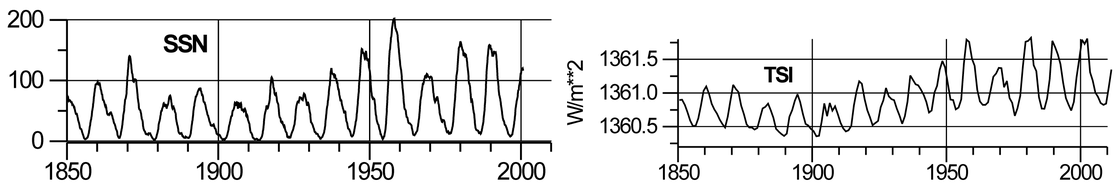

Figure 1: Variations of SSN, TSI

The N-SSA (Fig.2) is determined from the relation $(S_n - S_s)/(S_n + S_s)$, where the S_n and S_s are monthly sunspot area on the Northern and Southern solar hemispheres, respectively. The data since 1874 are observed by the Royal Greenwich Observatory and merged after 1976 with the US Air Force (USAF) and the US National Oceanic and Atmospheric Administration (NOAA) data by D. Hathaway. The variations of the value of Chandler period (Fig.3) are calculated by polar motion coordinates from the solution C01 of the IERS and the method, described in (Vondraák et al., 2005).

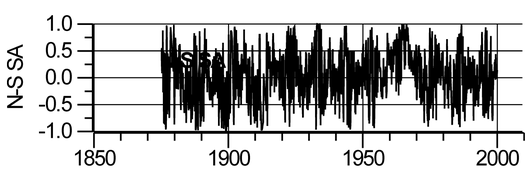

Figure 2: Variations ofN-SSA

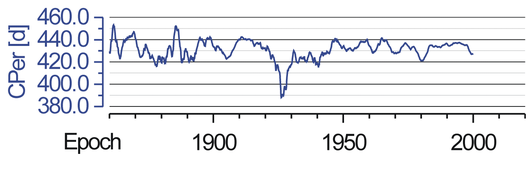

Figure 3: Variations the period of Chandler wobble, determined from the solution C01 of IERS.

The periodical variations are derived from the data by means of partial Fourier approximation based on the Least-Squares (LS) estimation of Fourier coefficients. The Partial Fourier approximation of discrete data is given by

$$F(t) = f_0 + f_1(t - t_0) + \sum_{k=1}^{n} a_k \sin \omega_k + b_k \cos \omega_k, \quad \text{where} \quad \omega_k = k\frac{2\pi}{P_0}(t - t_0)$$

and P_0 is the period of the first harmonic, t_0 – the mean epoch of observations, f_0, f_1, a_k and b_k are unknown coefficients and n is the number of harmonics of the partial sum, which covers all oscillations with periods between P_0/n and P_0. The application of the LS estimation of Fourier coefficients needs at least $2n + 2$ observations, so the number of harmonics n is chosen significantly smaller than the number N of sampled data f_i. The small number of harmonics n yields to LS estimation of the coefficient errors. This estimation is the first essential difference with the classical Fourier approximation. The second difference is the arbitrary choice of the period of first harmonic P_0, instead of the observational time span, so the estimated frequencies may cover the desired set of real oscillations. This method allows a flexible and easy separation of harmonic oscillations into different frequency bands by the formula

$$B(t) = \sum_{k=m_1}^{m_2} a_k \sin \omega_k + b_k \cos \omega_k \text{ and desired } \omega_k \text{ are in the bandwidth } \frac{2\pi m_1}{P_0} \le \omega_k \le \frac{2\pi m_2}{P_0}.$$

After estimating the Fourier coefficients, it is possible to identify a narrow frequency zone presenting significant amplitude, and defining a given cycle. Then this cycle can be reconstructed in time domain as the partial sum limited to the corresponding frequency bandwidth. Doing this for terrestrial and solar time series, we shall identify their respective cycles, isolate and compare the common ones.

Results and conclusions

The time series variations are separated in several interannual and decadal frequency bands by PFA with periods 3.4–3.5yr; 3.9–4.0yr; 6.2–6.5yr; 8.2–8.7yr; 10.4–11.2yr; 12.0–13.0yr; 15.6–17.3yr; 39–52yr and 78–156yr, where good correlation exists between solar indices and Chandler period variations. The long-term variations of the Chandler period are affected by N-S solar asymmetry (Fig.4), where the time lag is equal to the 22-year Hale magnetic solar cycle. Excellent agreement between TSI and Chandler period variations exists for oscillations with periodicities 39-52yr and all cycles with periods between 6 and 17 years (Figs. 5-10). The interannual oscillations with periods below 4 years are affected by the SSN variations (Figs. 11, 12). The CW grand minimum around 1930 is strongly connected with all solar harmonics with dominating influence of long term N-S SA variations (periodicity 78-156yr, CW period decrease - 6d) and TSI variations (periodicity 39-52yr, CW period decrease - 10d). The TSI influence on CW period variations is non-linear and frequency dependent. The value of CW period increase during the warming cycles of solar activity and decrease during some solar minima. This result means that the solar activity significantly affects the polar motion and CW variations by intermediate climatic variations in ocean and atmosphere.

References

Coddington, O., et al., 2015, Bull. American Meteorological Soc.

Kopp, G., et al., 2016, Solar Physics.

Lean, J.L.,2000, Geophysical Research Letters, 27, 16.

Lean, J.L., 2010, Wiley Interdisciplinary Reviews, Climate Change 1.

Vondrák, J., Ron, C., 2005, Cahiers du CEGS, 24, 39.

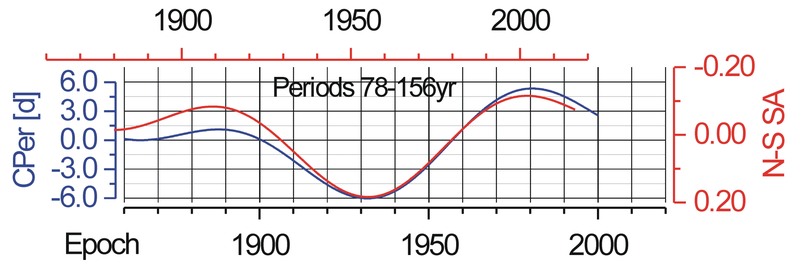

Figure 4: Influence of N-S solar asymmetry variations with periodicity 78-156yr on Chandler wobble.

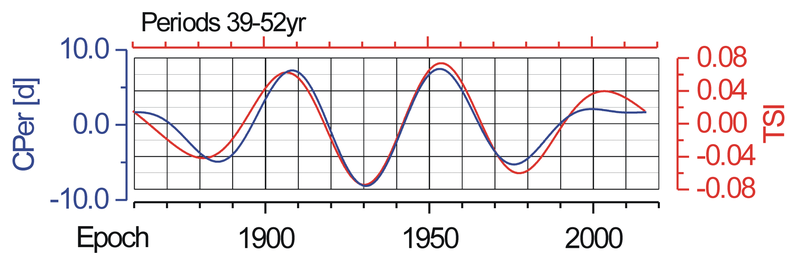

Figure 5: Influence of TSI variations with periodicity 39-52yr on Chandler wobble.

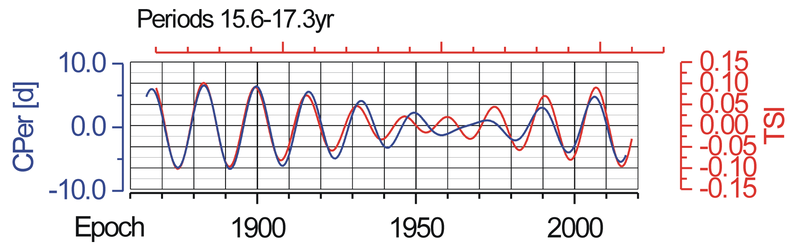

Figure 6: Influence of TSI variations with periodicity 15.6-17.3yr on Chandler wobble.

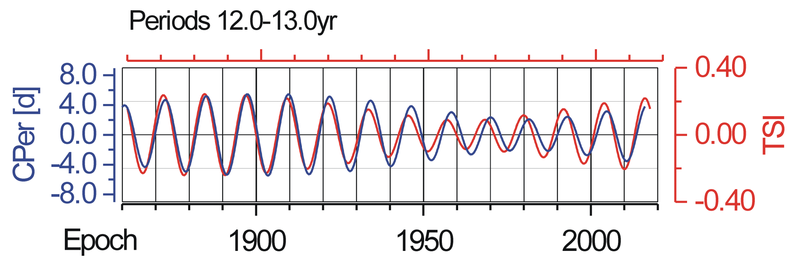

Figure 7: Influence of TSI variations with periodicity 12-13yr on Chandler wobble.

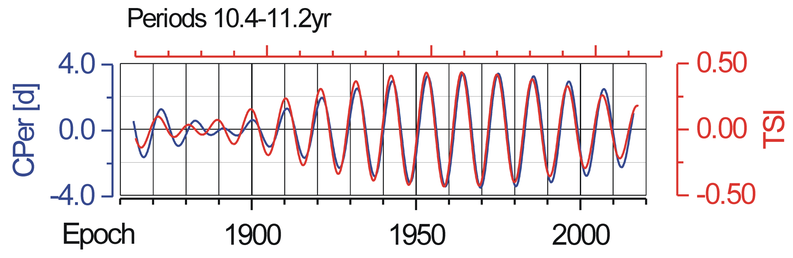

Figure 8: Influence of TSI variations with periodicity 10.4-11.2yr on Chandler wobble.

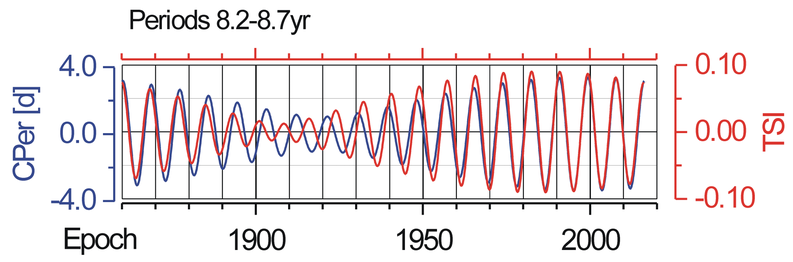

Figure 9: Influence of TSI variations with periodicity 8.2-8.7yr on Chandler wobble.

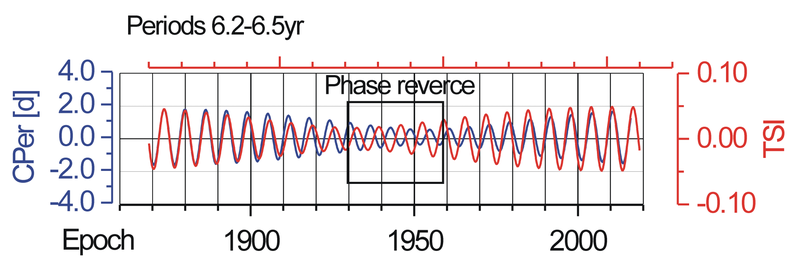

Figure 10: Influence of TSI variations with periodicity 6.2-6.5yr on Chandler wobble.

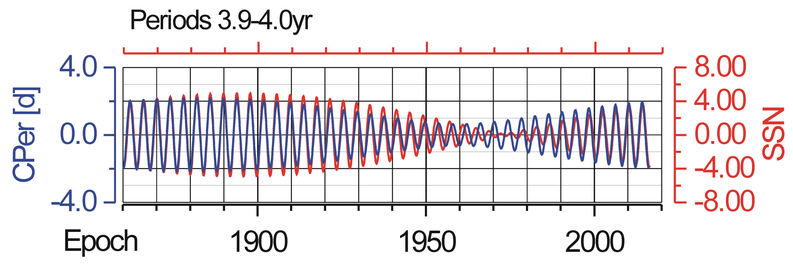

Figure 11: Influence of SSN variations with periodicity 3.9-4.0yr on Chandler wobble.

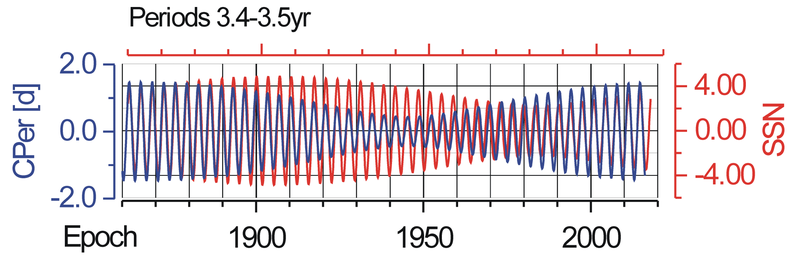

Figure 12: Influence of SSN variations with periodicity 3.4-3.5yr on Chandler wobble.